Late Quaternary micromammals and the precipitation history of the southern Cape, South Africa

J. Tyler Faith, Brian M. Chase, D. Margaret Avery

Late Quaternary micromammals and the precipitation history of the southern Cape, South Africa

J. Tyler Faith
Natural History Museum of Utah & Department of Anthropology
University of Utah
Salt Lake City, UT 84108 USA
E-mail: jfaith@nhmu.utah.edu; Telephone: (801) 581-8572

Brian M. Chase
Centre National de la Recherche Scientifique
Institut des Sciences de l'Evolution de Montpellier
Université Montpellier
34095 Montpellier, France
E-mail: brian.chase@univ-montp2.fr

D. Margaret Avery
Iziko South African Museum
P.O. Box 61
Cape Town, 8000 South Africa
E-mail: mavery@iziko.org.za

Manuscript draft: June 7, 2018

ABSTRACT

The southern Cape of South Africa is important to understanding regional climate because it straddles the transition between the winter and summer rainfall zones. We examine late Quaternary changes in rainfall seasonality and aridity through analysis of micromammal assemblages from three sites: Boomplaas Cave and Nelson Bay Cave in the aseasonal rainfall zone, and Byneskranskop 1 in the winter rainfall zone. Our interpretation is based on analysis of 123 modern micromammal assemblages accumulated by barn owls (*Tyto alba*), which empirically links species composition to climate. The Pleistocene record (~65 to 12 ka) from Boomplaas Cave, together with the Last Glacial Maximum (LGM) samples from Nelson Bay Cave, indicates enhanced winter rainfall, especially during the LGM. Boomplaas Cave documents progressive aridification from the LGM to the earliest Holocene, followed by a return to moderately humid conditions through the Holocene.. Byneskranskop 1 indicates a dominance of winter rains over the last 17 ka, and a shift from an arid middle Holocene to a humid later Holocene. Agreement between the micromammal record and other local and regional proxies reinforces the potential of southern African micromammal assemblages as paleoclimate indicators.

Keywords: Aridity, Holocene, Last Glacial Maximum, Mammals, Paleoclimate, Precipitation, Seasonality

INTRODUCTION

The southern Cape of South Africa, here defined as the region encompassing the southern coastal plains and the east-west trending ranges of the Cape Fold Belt, straddles the transition between the winter rainfall zone (WRZ; > 66% of mean annual precipitation falls from April to September) to the west and the summer rainfall zone (SRZ; >66% of mean annual precipitation falls from October to March) to the east (sensu Chase and Meadows, 2007; Fig. 1). The WRZ receives most of its rainfall from the frontal systems associated with the westerly storm track, which migrates northward during the austral winter. In contrast, precipitation in the SRZ is related to tropical easterly flow, which advects moisture from the Indian Ocean during the summer months (Tyson, 1986; Chase and Meadows, 2007). Because most of the southern Cape falls within the aseasonal rainfall zone (ARZ; Fig. 1), receiving precipitation throughout the year from both sources and their combined effects (Chase et al., 2017, 2018) , the region is uniquely positioned to inform on the history of these temperate and tropical circulation systems.

Quaternary variability in these two systems in southern Africa has been a focus of research for decades (van Zinderen Bakker, 1967, 1976; Heine, 1982; Cockcroft et al., 1987; Deacon and Lancaster, 1988). The dominant paradigm suggests that the boundaries of the WRZ and SRZ have shifted through time, due to the enhancement of winter rainfall during glacials and enhancement of summer rainfall during interglacials (see reviews in Deacon and Lancaster, 1988; Partridge et al., 1990; Chase and Meadows, 2007; Chase et al., 2017). However, the precipitation history of the southern Cape remains unclear and debated. For instance, cool phases of the Pleistocene have

been associated with enhanced winter rains (Faith, 2013b; Sealy et al., 2016; Chase et al., 2018), whereas some records link cool conditions to intensified summer rains (Bar-Matthews et al., 2010). Even the most basic particulars—were glacials wetter or drier than interglacials?—are uncertain (Chase and Meadows, 2007; Marean et al., 2014), with some, for example, characterizing the Last Glacial Maximum (LGM: 26.5-19 ka; Clark et al., 2009) as harsh and arid (e.g., Avery, 1982; Deacon et al., 1984; Deacon and Lancaster, 1988) or humid and highly productive (e.g., Faith, 2013b; Chase et al., 2017, 2018). Uncertainty in these and other aspects of the region's precipitation history stems in part from a lack of records that inform directly on the relevant climate parameters (Chase et al., 2013). This is exacerbated by a combination of seemingly contradictory lines of evidence (e.g., Avery, 1982, 2004), conflicting interpretations of the evidence (e.g., Deacon et al., 1984; Faith, 2013a), and a substantial degree of not yet well-understood spatial variation (Chase et al., 2015b; Chase et al., 2017), such as evidence indicating that coastal archives are out of phase with those found in the interior (Chase and Quick, 2018).

Of the various proxy records from the southern Cape (reviewed in Chase and Meadows, 2007; Marean et al., 2014), the fossil record of raptor-accumulated micromammal assemblages from cave deposits features prominently in discussion of past climate and environment (e.g., Avery, 1982, 1983; Deacon et al., 1984; Avery, 1987; Thackeray, 1987; Avery, 1990; Thackeray, 1990; Avery, 1993, 2004; Matthews et al., 2011; Nel and Henshilwood, 2016; Nel et al., 2018; Thackeray and Fitchett, 2016). Such assemblages are widely used to inform on climate in a diverse range of geographic and temporal settings (e.g., Andrews, 1990), though interpretations of those

from the southern Cape are, like other records from the region, not always in agreement (e.g., Avery, 1982; Thackeray, 1987; Avery, 2004; Faith, 2013a). Our aim here is to revisit several key late Quaternary micromammal sequences, with a focus on their implications for the region's precipitation history. The main contribution of this study is that our interpretations are informed by a large sample of modern micromammal assemblages from southern Africa. We use these assemblages to relate variation in taxonomic composition to variation in climate, which provides an empirical framework for interpreting taxonomic fluctuations in the past.

MATERIALS AND METHODS

Micromammal assemblages

Our analysis makes use of taxonomic abundance data—quantified according to the minimum number of individuals (MNI) after Avery (1982)—from modern and fossil micromammal assemblages. The species included in our analysis typically weigh less than 150 grams and include rodents (Rodentia), shrews (Soricidae), elephant shrews (Macroscelididae), and golden moles (Chrysochloridae). The taxonomy used here follows Wilson and Reeder (2005). Bats are not considered in our analysis.

The modern sample includes 123 assemblages collected by D.M.A. from barn owl (*Tyto alba*) roosts across southern Africa (Fig. 1) (see Avery, 1999), and currently curated at the Iziko South African Museum in Cape Town (Supplementary Tables 1-2). At each sample locality, whole or partial barn-owl pellets were collected and, where appropriate, bulk debris from collapsed pellets was bagged for subsequent analysis. Some assemblages, such as those from West Coast National Park (Avery, 1992), were

sampled multiple times. Assemblage sample size ranges from 24 to 6943 individuals (median = 243.5). Important to our work here, these assemblages encompass a broad range of precipitation regimes (from 19-91% summer rain), occurring in the SRZ (n = 60), the WRZ (n = 41), and in the ARZ (n = 22). Following the UNEP (United Nations Environment Programme) (1997) classification scheme for aridity, sites are characterized by climates that are arid (n = 41), semi-arid (n = 52), dry sub-humid (n = 28), and humid (n = 2) (Fig. 2). We caution that the small sample of assemblages from humid climates limits our ability to model the relationship between species composition and climate at the more humid end of the spectrum.

Fossil data are derived from Avery (1982) and include the late Quaternary assemblages from three southern Cape archaeological sites: Boomplaas Cave (Deacon, 1979) and Nelson Bay Cave in the ARZ (Klein, 1972; Deacon, 1984) and Byneskranskop 1 (Schweitzer and Wilson, 1982) in the WRZ (Fig. 1). These sites were selected to the exclusion of a few others from the region (e.g., Die Kelders and Klasies River) because of their more robust chronologies (Loftus et al., 2016; Pargeter et al., 2018), and because they include deposits sampling the transition from glacial to interglacial conditions. Located on the southern flanks of the Swartberg range ~80 km inland, Boomplaas Cave was excavated by Hilary Deacon in the 1970s (Deacon, 1979; Deacon, 1984). It provides the longest sequence examined here, spanning the last ~65 ka, with a particularly well-dated sequence after the onset of the LGM (Pargeter et al., 2018). Nelson Bay Cave is located on the Robberg Peninsula on the southern Cape coastline. It was excavated by Ray Inskeep (1987) and later by Richard Klein (1972; see also Deacon, 1984). Microfauna data are only available from layers YSL and

YGL (Klein's excavation), dating to 23.5-21.0 ka and 22.1-16.3 ka, respectively (Loftus et al., 2016). Lastly, Byneskranskop 1 is located at the western margin of the southern Cape, ~7 km from the modern coastline. Excavations by Franz Schweitzer in the 1970s (Schweitzer and Wilson, 1982) uncovered a stratified sequence spanning the last 17 ka (Loftus et al., 2016). The stratigraphy, chronology, and taxonomic abundance data for each of the assemblages examined here are reported in Supplementary Table 3.

Details concerning the taphonomic histories of the fossil assemblages require that we make a few assumptions. First, we note that the microfauna from Boomplaas Cave were recovered using a combination of 2- and 3-mm mesh, whereas 3-mm mesh was used for the other two sites. Because finer mesh was not used at any site, there is potential for taphonomic bias against recovery of smaller specimens and smaller-bodied species (e.g., Lyman, 2012). We assume that the effects of such bias are consistent within a given site. In addition, we must also make an assumption about the accumulator(s) of the micromammal remains. Avery (1982) argued that barn owls were the primary accumulators of the microfauna from all three sites. This inference was based on assessment of the ecology of potential accumulators and the represented prey species, as her analysis was conducted before development of taphonomic approaches for identifying the likely bone accumulators (e.g., Andrews, 1990). However, there is reason to believe that other raptor species could have accumulated some of the microfaunal remains examined here. For example, taphonomic analysis of the macrofauna from Boomplaas Cave indicates that some of the smaller species (e.g., leporids, hyraxes, smaller ungulates) were accumulated by very large raptors (Faith, 2013a). Likewise, spotted eagle owls (*Bubo africanus*) are implicated in the taphonomic

167 histories of other microfaunal assemblages from the region (Matthews et al., 2011; Nel
168 et al., 2018), though they generate microfaunal assemblages that are very similar in
169 composition to those of barn owls (Reed, 2005). In the absence of taphonomic analysis
170 of the micromammal assemblages, we assume that contributions by other bone
171 accumulators have not overprinted the environmental signal in a manner that would
172 substantially alter our results.

173 Barn owl assemblages are usually though to provide a reasonably accurate
174 representation of the local micromammal community (e.g., Andrews, 1990; Fernández-
175 Jalvo et al., 2016). They typically forage within a radius of up to 2-3 km (Andrews,
176 1990), preferentially targeting open habitats where it is easier to locate and capture prey
177 (Taylor, 1994). The relatively small foraging radius implies that the modern and fossil
178 assemblages examined here provide highly localized samples of the micromammal
179 community. It follows that they may be especially sensitive to local environmental
180 conditions. This spatial scale must be considered when interpreting micromammal
181 assemblages in terms of much larger-scale climate phenomena (see Discussion). The
182 open-habitat bias is less of a concern here, as it is likely to be consistent across all
183 assemblages.

184

185 **Analytical methods**

186 For each of the 123 modern micromammal assemblages, we extracted data on rainfall
187 seasonality and aridity from the WorldClim global climate database (Hijmans et al.,
188 2005) and from the Global Aridity Index database (Zomer et al., 2007; Zomer et al.,
189 2008; Trabucco and Zomer, 2009). Though there is a recent update to WorldClim

(WorldClim 2: Fick and Hijmans, 2017), we use the original because it provides the basis for the data modelled in the Global Aridity Index database. We calculated three complementary measures of rainfall seasonality from the WorldClim database: the percentage of annual precipitation that falls (1) during the coolest quarter of the year (%cold-quarter rainfall: June, July, August), (2) during the warmest quarter of the year (%warm-quarter rainfall: December, January, February), and (3) during the warmest half of the year (%summer rainfall: October through March). The aridity index (AI) reported in the Global Aridity Index database is expressed as:

$$AI = MAP / MAE$$

where MAP is mean annual precipitation and MAE is mean annual evapotranspiration. Higher AI values indicate more humid conditions. While MAP is strongly correlated with AI in our dataset ($r = 0.958$, $p < 0.001$), we focus on AI because many climate proxies, including flora and fauna, are more directly influenced by moisture availability (humidity/aridity) rather than the total amount of precipitation (e.g., Chevalier and Chase, 2016). It is important to note, however, that while AI can be calculated at broad spatial scales, moisture availability is usually much more heterogeneous than these calculations suggest. Even modest topographic variability can significantly disperse or concentrate surface and groundwater resources, creating substantial micro-topographical differences in moisture availability within regions of similar MAP/MAE.

We use canonical correspondence analysis (CCA) to relate the taxonomic composition of the modern assemblages to precipitation seasonality (%warm-quarter

and %cold-quarter rainfall) and aridity. CCA is a constrained ordination approach in which faunal assemblages are ordinated relative to one or more known environmental variables, and the species abundances are considered a response to the environmental gradient (Legendre and Legendre, 2012). When the primary axes are plotted in a bivariate plot, assemblages from similar climate regimes will plot close to each other, and the species will plot nearest to those assemblages in which they are most abundant. We then input the Quaternary fossil assemblages into the CCA as supplementary points; these are points that are projected in the same multivariate space as the modern assemblages, but they have no influence on the original ordination. Because the ordination of modern assemblages in the CCA is designed to track environmental variables (the extent to which this is so is examined below), this allows us to interpret ordination scores of fossil assemblages in terms of precipitation seasonality and aridity. We exclude singleton taxa (i.e., those that occur in only one assemblage) from the analysis, as they can disproportionately influence the ordination (Legendre and Legendre, 2012). All fossil assemblages with sample sizes greater than 10 individuals are included in the analysis (assemblage LOH from Boomplaas Cave and Layer 3 from Byneskranskop 1 are excluded).

The use of CCA allows us to consider the environmental implications of all taxa simultaneously, in contrast to traditional paleoenvironmental inferences derived from (potentially subjective) interpretations of a select handful of indicator taxa. However, it is important to note an assumption that is central to our approach, or indeed any technique that links the taxonomic composition of faunal assemblages to climate or environment. We assume that the target variables (rainfall seasonality and aridity) are

236 important determinants of taxonomic composition (e.g., Birks, 1995). Violation of this
237 assumption translates to reduced accuracy of the environmental reconstruction (e.g., Le
238 and Shackleton, 1994). Though our primary interests concern aridity and rainfall
239 seasonality, we recognize that the presence and abundance of a species in a given
240 assemblage is likely mediated by multiple climatic or environmental variables. For
241 example, some species may indicate highly localized environments (e.g., dense
242 vegetation along a water course) irrespective of variation in our target environmental
243 variables. To enhance compliance with this assumption, we implemented a protocol to
244 ensure analysis of those taxa that are relatively unambiguous indicators of rainfall
245 seasonality or aridity. In particular, we eliminated taxa that are often found in both
246 winter- or summer-dominated rainfall regimes and in relatively humid or arid climates.
247 To do so, we calculated the interquartile range (IQR: 25^{th} to 75^{th} percentile) of
248 %summer rainfall and AI values that characterize the modern assemblages in which a
249 given taxon is found (see Supplemental Table 3). We excluded those taxa (n = 16)
250 whose IQRs encompass intermediate values of rainfall seasonality and aridity, defined
251 here as 50% summer rainfall and an AI value of 0.40; the former represents the
252 threshold separating assemblages that receive more winter or more summer rainfall,
253 and the latter represents the midpoint of the range of AI values in the modern sample
254 (from 0.05 to 0.75). Not only are the excluded taxa ambiguous indicators of our target
255 environmental variables (e.g., because they occur in relatively humid or arid climates),
256 but they also tend to have relatively broad tolerances with respect to rainfall seasonality
257 and aridity. The median IQRs of %summer rainfall (46%) and AI values (0.29) of
258 excluded taxa are considerably larger than those of taxa included in analysis (%summer

rainfall: 16%; AI: 0.14). In other words, excluded taxa are found in modern assemblages characterized by a much broader range of seasonality and AI values than those retained for analysis.

Though it is possible to use these and related analytical approaches to generate numerical reconstructions of past climate (e.g., the aridity index at time X was 0.45) (Birks, 1995), we emphasize ordinal-scale trends here (e.g., more/less arid) to avoid generating results that are seemingly precise but potentially inaccurate. There are several reasons for doing so. First, our assumptions concerning the taphonomic histories of the fossil assemblages reinforce the need for conservative interpretation of the fossil data. Second, taxonomic abundances from fossil mammal assemblages—typically quantified according to MNI or the number of identified specimens (NISP)—often behave in a manner that is ordinal-scale (Grayson, 1984; Lyman, 2008). And lastly, we note that the analyzed fossil assemblages are time-averaged by amounts ranging from hundreds to thousands of years. The precision implied by numerical paleoclimate reconstructions is of questionable accuracy considering that the relatively coarse temporal resolution of the fossil assemblages means they are likely to sample short-term climatic fluctuations. It is for this reason—specifically, the need to ensure that we ask paleoclimatic questions that can be answered given the temporal resolution of the fossil data (e.g., Lyman, 2017)—that we also emphasize long-term paleoclimatic trends (e.g., from the LGM to the onset of the Holocene), highlighting shorter-term climate phenomena only when we have sufficient resolution to do so.

RESULTS

Modern assemblages

Figure 3 plots the ordination of sites and species along the first two axes of the CCA. For the sake of clarity, site names are omitted and they are instead coded by precipitation regime (WRZ, SRZ, and ARZ) and UNEP aridity classification (arid, semi-arid, dry sub-humid, humid). Only those species present in the fossil assemblages are illustrated here. Full details concerning the CCA ordination scores for sites and taxa are provided in Supplementary Table 4.

The first axis (axis 1) accounts for 54.8% of the inertia (~variation in taxonomic composition), and it broadly tracks precipitation seasonality. Sites and species with negative values are associated with a greater percentage of warm-quarter rainfall and those with positive values are associated with a greater percentage of cold-quarter rainfall. This relationship is further illustrated in Figure 4A, which plots the axis 1 scores for a given site against %summer rainfall. There is a strong and significant inverse correlation between the two variables ($r = -0.880$, $p < 0.001$). The second axis of the CCA accounts for 45.1% of the inertia and tracks the aridity index (Fig. 3). Sites and species associated with more humid environments tend to have negative axis 2 scores, whereas those associated with arid settings tend to have positive axis 2 scores. This is also shown in Figure 4B, which plots axis 2 scores against the logarithm of the aridity index. The correlation is strong and highly significant ($r = -0.859$, $p < 0.001$).

Fossil assemblages

The previous analysis indicates that we can use the ordination of assemblages along the first two axes to track ordinal-scale change in rainfall seasonality and aridity in the fossil record. Figure 5 plots the fossil assemblages in the same multivariate space as the modern assemblages. Though sample size can potentially influence such analyses because larger samples translates to recovery of more species (Grayson, 1984; Lyman, 2008), which could potentially include species with a disproportionate effect on the ordination, this is not the case here; for the two sites with long stratified microfaunal sequences (Boomplaas and Byneskranskop 1), assemblage sample size is not related to axis 1 and 2 scores (Spearman's rho: $p > 0.15$ for all correlations).

Boomplaas Cave

The Boomplaas Cave assemblages show substantial variation along both axes (Figs. 5-7). From the base of the sequence to the end of the LGM (layer GWA), increasing axis 1 scores suggests increasing winter rainfall (Spearman's rho: $r_s = -0.857$, $p = 0.007$). Axis 2 scores remain relatively low (= humid) and stable at this time. The last glacial-interglacial transition (LGIT: layers CL3 to BRL6) is associated with considerably lower axis 1 scores and a significant temporal increase in axis 2 scores ($r_s = 1.000$, $p = 0.017$), suggesting enhanced summer rainfall and increasing aridity relative to the LGM. The shift towards more arid conditions peaks in the earliest Holocene (BRL5), with conditions becoming more humid thereafter (declining axis 2 scores from BRL5 to DGL: $r_s = -1.000$, $p < 0.001$). The increase in humidity through the Holocene is associated

with increased influence of summer rains (declining axis 1 scores from BRL5 to DGL: –0.893, $p = 0.012$).

Nelson Bay Cave

The availability of only two assemblages from Nelson Bay Cave precludes an analysis of temporal change, but they do speak to LGM conditions on the south coastal plains—though the coastline was far from the site at this time (Van Andel, 1989; Fisher et al., 2010)—relative to the other fossil samples. As indicated in Figure 5, both assemblages from this site have positive axis 1 scores that are comparable to or greater than the LGM assemblages from Boomplaas and those from Byneskranskop 1. Though we lack a Holocene comparison from Nelson Bay Cave, this is consistent with enhanced winter rains during the LGM, especially considering the similarities in axis 1 scores with a south coast site that is today in the WRZ (Byneskranskop 1). The axis 2 scores are more positive than those from the LGM at Boomplaas Cave, implying drier conditions on the south coastal plains relative to the Swartberg range.

Byneskranskop 1

The Byneskranskop 1 assemblages show relatively muted variation along the first and second axes of the CCA (Figs. 5-7). There are no clear directional changes across the LGIT (Layers 19-15; Fig. 6), though there is considerable variation within the Holocene (Figs. 6, 7). This variation includes a brief humid pulse associated with increased influence of summer rainfall in the earliest Holocene (Figs. 6, 7). We also observe a steady and statistically significant increase in humidity (declining axis 2 scores: r_s = –

0.900, $p < 0.001$) coupled with increasing summer rainfall (declining axis 1 scores: $r_s = -0.636$, $p = 0.032$) from layer 12 (~8.5 kcal BP) through to the top of the sequence. To the extent that the uppermost assemblage signals climates similar to the present, we infer that the influence of summer rainfall has been similar to or less than today, implying dominance of winter rainfall throughout the last 17 ka.

DISCUSSION

Our analyses differ from previous studies of southern Cape micromammal assemblages in that they are informed by a large sample of modern assemblages, which provides an empirical link between taxonomic composition and climate (see also Campbell et al., 2011; Campbell et al., 2012). The strong relationships between taxonomic composition and climate documented in our analysis (Fig. 4) enhance confidence that our interpretations of the fossil record are reflecting changes in the target environmental variables. Particularly important are the high coefficients of determination (r^2) for the correlations involving rainfall seasonality (axis 1 and %summer rainfall: $r^2 = 0.775$) and aridity (axis 2 and AI: $r^2 = 0.738$), which together imply that the majority of variance in taxonomic composition of the modern assemblages is related to the target climatic variables. It follows that even though barn owl assemblages provide highly localized representations of the micromammal community (within a 2-3 km radius), they are still highly sensitive to larger-scale climate parameters, at least over the spatial scales examined here. Though the microfaunal record is not as well-resolved as some other

climate records from the region, namely those provided by hyrax middens (e.g., Chase et al., 2015b, 2018), speleothems (e.g., Talma and Vogel, 1992), and lake cores (e.g., Quick et al., 2015, 2016), it does provide a valuable, and compared to many archives, unique, opportunity to simultaneously explore shifts in both moisture availability and rainfall seasonality.

Change in the ARZ

The Boomplaas Cave record contributes to an increasingly coherent picture concerning late Quaternary variation in temperate (winter rains) and tropical (summer rains) precipitation systems in what is today the ARZ. It attests to increasing influence of winter rains after ~60 ka, with the strongest winter rainfall signal occurring immediately before and during the LGM (Fig. 6). The Nelson Bay Cave record is consistent with this trend, providing a strong winter rainfall signal in the two samples dating from 23.5 to 16.3 kcal BP (Fig. 5).

Enhanced winter rains during the LGM is consistent with recent inferences derived from the Boomplaas microfauna (Thackeray and Fitchett, 2016) and with stable carbon ($\delta^{13}C$) isotopes from Boomplaas grazers (Sealy et al., 2016). The latter indicate abundant C_3 grass during the LGM; because the proportion of C_3 and C_4 grasses in South Africa tracks the influence of winter and summer rains (Vogel et al., 1978), this is consistent with greater influence of winter rainfall. Likewise, the expansion of grassland implied by the Boomplaas micromammals (Avery, 1982) and larger mammals (Klein, 1983; Faith, 2013a), together with the strong C_3 signature in the nearby (~3 km east) Cango Caves speleothem (Talma and Vogel, 1992), is also indicative of abundant C_3

grasses and winter rains at this time. Further afield at Seweweeksport, in the Swartberg range 70 km west of Boomplaas (Fig. 1), the combination of elevated grass pollen and reduced $\delta^{13}C$ in a series of hyrax middens suggests that most rain fell during the winter (Chase et al., 2017, 2018) (Fig. 7D). A potential discrepancy is provided by Sealy's (1996) analysis of $\delta^{13}C$ in grazers from Nelson Bay Cave. She interpreted stasis in the $\delta^{13}C$ values of *Syncerus caffer* and *Hippotragus* spp. through the sequence as evidence for stability in the influence of summer and winter rainfall regimes. However, we note that this signal may be influenced by east-west migration of ungulate grazers along the paleo-Agulhas plain during the LGM (Marean, 2010; Faith and Thompson, 2013, Copeland et al., 2016), which would imply that their $\delta^{13}C$ signatures are not indicative of local vegetation or rainfall regimes.

.

At Boomplaas Cave, the LGIT (CL3 to BRL6) is associated with enhanced summer rainfall relative to the LGM. (Fig. 6). This is also evident in the Seweweekspoort $\delta^{13}C$ record, which documents an increase in C_4 vegetation through the LGIT (Fig. 7D). The increasing influence of summer rains broadly tracks changes in summer rainfall inferred from a recent statistical analysis of pollen archives in the interior (SRZ) of southern Africa (Chevalier and Chase, 2015) (Fig. 7A). At the same time, the declining influence of winter rains also tracks the decline in Antarctic sea-ice extent inferred from sea salt sodium flux from the EDML ice core (Fischer et al., 2007; Fig. 7H), consistent with the hypothesis that winter rains are linked to the expansion and contraction of Antarctic sea ice and its effect on the position of the southern westerlies (e.g., van

Zinderen Bakker, 1976; Stuut et al., 2004; Chase and Meadows, 2007; Chase et al., 2013, 2017).

In contrast to the coherent picture concerning rainfall seasonality provided by southern Cape paleoclimate archives, there is substantial disagreement about variation in moisture availability from the ARZ (e.g., Avery, 1982; Deacon et al., 1984; Scholtz, 1986; Deacon and Lancaster, 1988; Avery, 2004; Chase and Meadows, 2007; Faith, 2013a, b; Chase et al., 2017, 2018). Our results contribute to a growing body of evidence suggesting a transition from a relatively humid LGM to a more arid Holocene (e.g., Faith 2013a, b; Chase et al., 2017, 2018). The increase in aridity from the LGM to the early Holocene at Boomplaas Cave (Fig. 7C) broadly parallels the $\delta^{15}N$ record from the Seweweekspoort hyrax middens (Chase et al., 2017, 2018; Fig. 7E). These records are out of phase with the pollen-derived precipitation record from the SRZ (Chevalier and Chase, 2015; Fig. 7A), consistent with the expected inverse relationship between temperate and tropical systems over orbital time-scales (Chase et al., 2017).

The relatively humid conditions observed during the LGM persist until ~15 ka, with conditions becoming increasingly arid thereafter (Fig. 6, 7C). We argue that increased evapotranspiration due to warmer temperatures is largely responsible for aridification from 15 ka to the end of the Pleistocene (Fig. 7C). This is suggested by a lack of evidence for changes in rainfall seasonality at Boomplaas Cave (Fig. 7B), together with an absence of prominent directional shifts in SRZ precipitation (Fig. 7A) or Antarctic sea ice (Fig. 7H) over this interval, implying little net change in the strength of tropical or temperate precipitation systems. The aridification trend peaks in the earliest Holocene (Fig. 6, 7C), which represents the most arid portion of the sequence. There is

no evidence in the Boomplaas Cave record for the humid pulse seen at Seweweekspoort at ~11 ka (Fig. 7E), but in the absence of better age control for the early Holocene portion of the sequence we cannot rule out the possibility that Boomplaas lacks deposits that sample this relatively short-lived episode or that time-averaging may have muted the signal.

The phase of early Holocene aridity documented in the micromammal record is followed by increasingly humid conditions coupled with a moderate increase in the proportion of summer rain (Fig. 6). The Seweweekspoort $\delta^{15}N$ record lacks a comparable directional change in moisture availability, but it does indicate an increase in grass pollen (Chase et al., 2018) in conjunction with a stronger C_4 signature from the early Holocene until ~ 2 ka (Fig. 7D). An increase in C_4 grasses is also evident in the Cango Caves speleothem for the latter half of the Holocene (there is no record for the first half) (Talma and Vogel, 2013). The combination of evidence from these three archives implies enhanced summer rainfall in the region. Greater rainfall in the warmest portion of the year is likely to promote expansion of shallow-rooting vegetation, including C_4 grasses. Why this increase in summer rainfall is associated with greater humidity at Boomplaas but not at Seweweekspoort is not immediately clear. Resolving this discrepancy will require, among other things, additional records from the ARZ.

Change in the WRZ

The Byneskranskop 1 micromammals provide relatively little evidence for major changes in rainfall seasonality (e.g., compared to Boomplaas Cave), implying a dominance of winter rains over the last 17 ka (Fig. 6). This is not surprising given that the site is located far west of the Indian Ocean moisture source responsible for summer

rains. In terms of both seasonality and aridity, there are no clear directional changes across the LGIT (Layers 16-19: Fig. 6). Rather, changes within the Holocene (Layers 15-1) are more pronounced than those occurring across the Pleistocene-Holocene transition. The earliest Holocene (Layer 14) is associated with humid conditions (low axis 2 scores), corresponding closely with a similar humid pulse documented in the Seweweekspoort record (Chase et al., 2017, 2018), where it dates from 11.8 to 10.7 kcal BP (Fig. 9E). The mechanisms underpinning this humid phase have been suggested to relate to an increase in tropical influence (Chase et al., 2017), and this is clearly reflected in the micromammalian assemblage by reduced axis 1 scores (Figs. 8, 9).

Following the brief humid phase in the earliest Holocene, we observe a relatively arid middle Holocene—with the driest conditions occurring in Layer 12 (8.7-8.3 ka)—followed by a gradual return to more humid conditions thereafter (Fig. 6, 7). This arid phase has been attributed to reduced influence of the westerlies (Chase et al., 2017), and numerous records from elsewhere in the WRZ also suggest that the middle Holocene was more arid than what came after (e.g., Klein, 1991; Meadows et al., 1996; Meadows and Baxter, 2001; Chase and Thomas, 2007; Scott and Woodborne, 2007b, a; Klein and Cruz-Uribe, 2016). Avery (1993) previously linked expansion of grasses during the middle Holocene to a less seasonal rainfall regime (i.e., a greater proportion of summer rains), but this is not evident in our analysis, which implies that summer rains were relatively unimportant at this time (Fig. 7F). Though it has been suggested that cooler temperatures and increased westerly influence may account for the more humid late Holocene (e.g., Chase and Meadows, 2007), more recent evidence (Chase et al.,

2017) indicates a decrease in westerly influence, and drier conditions at some WRZ sites (Chase et al., 2015a). At Byneskranskop 1, the shift towards mesic conditions beginning ~8 ka (Fig. 7G) is associated with (slightly) greater influence of summer rainfall (Fig. 7F), potentially translating to a less severe summer drought. This is consistent with evidence and inferences drawn from hyrax midden data from the eastern WRZ at Katbakkies Pass (Fig. 1), which indicate that although most rain falls in the winter, variation in overall moisture availability/drought stress is largely determined by the changing influence of summer rains and their effect on the severity of the dry season (see Chase et al., 2015b).

CONCLUSIONS

We show that the taxonomic composition of southern African owl-accumulated micromammal assemblages is strongly related to precipitation seasonality and aridity. We use these relationships to infer changes in the late Quaternary precipitation history of the southern Cape from three fossil assemblages. In what is today the ARZ, the micromammal records from Boomplaas Cave and Nelson Bay Cave imply enhanced winter rainfall during glacial Pleistocene, consistent with models suggesting eastward expansion of the WRZ (e.g., van Zinderen Bakker, 1976; Chase and Meadows, 2007; Chase et al., 2017). The Boomplaas Cave record contributes to a growing body of evidence implying a relatively humid LGM, followed by increased aridity across the LGIT.. The WRZ record from Byneskranskop 1 is characterized by relatively little change in rainfall seasonality throughout its sequence. Changes in moisture availability are more pronounced, however, especially during the Holocene. This includes a

relatively humid late Holocene, interrupted by a period of aridity during the middle Holocene, consistent with other records from the WRZ. Overall, the coherence between the micromammal record and other local and regional climate proxies (Figs. 9, 10) reinforces the abundant potential of southern African micromammal assemblages as indicators of paleoclimate (Avery, 1983, 1990, 2007). Although generation of new climate archives will be essential to resolving current and emerging questions concerning southern Africa's precipitation history, our analyses show that new analysis of the existing records can also help us get closer to the answers we seek.

ACKNOWLEDGMENTS

An early version of this study was presented at a Society for American Archaeology session organized by Eugene Morin, Arianne Boileau, and Elspeth Ready. The version reported here benefited from several participant comments. We thank the members of the University of Utah Archaeological Center, Curtis Marean (Associate Editor), and two anonymous referees for valuable feedback on an earlier draft. Justin Pargeter kindly shared new radiocarbon dates for Boomplaas Cave prior to their publication. An Australian Research Council (ARC) Discovery Early Career Researcher Award (DE160100030) supported JTF in the early stages of this project.

REFERENCES

Andrews, P., 1990. Owls, Caves, and Fossils. University of Chicago Press, Chicago.

530 Avery, D.M., 1982. Micromammals as palaeoenvironmental indicators and an
531 interpretation of the late Quaternary in the southern Cape Province, South Africa.
532 Annals of the South African Museum 85, 183-374.
533 Avery, D.M., 1983. Palaeoenvironmental implications of the small Quaternary mammals
534 of the fynbos region, In: Deacon, H.J., Hendey, Q.B., Lambrechts, J.J.N. (Eds.),
535 Fynbos Palaeoecology: A Preliminary Synthesis, South African National Scientific
536 Programmes Report No 75. Mills Litho, Cape Town, pp. 139-155.
537 Avery, D.M., 1987. Late Pleistocene coastal environment of the southern Cape Province
538 of South Africa: micromammals from Klasies River Mouth. Journal of Archaeological
539 Science 14, 405-421.
540 Avery, D.M., 1990. Holocene climatic change in southern Africa: the contribution of
541 micromammals to its study. South African Journal of Science 86, 407-412.
542 Avery, D.M., 1992. Ecological data on micromammals collected by barn owls *Tyto alba*
543 in the West Coast National Park, South Africa. Israel Journal of Zoology 38, 385-
544 397.
545 Avery, D.M., 1993. Last Interglacial and Holocene altithermal environments in South
546 Africa and Namibia: micromammalian evidence. Palaeogeography,
547 Palaeoclimatology, Palaeoecology 101, 221-228.
548 Avery, D.M., 1999. A preliminary assessment of the relationship between trophic
549 variability in southern African Barn owls *Tyto alba* and climate. Ostrich 70, 179-186.
550 Avery, D.M., 2004. Size variation in the common molerat *Cryptomys hottentotus* from
551 southern Africa and its potential for palaeoenvironmental reconstruction. Journal of
552 Archaeological Science 31, 273-282.

553 Avery, D.M., 2007. Micromammals as palaeoenvironmental indicators of the southern
554 Afrian Quaternary. Transactions of the Royal Society of South Africa 62, 17-23.
555 Bar-Matthews, M., Marean, C.W., Jacobs, Z., Karkanas, P., Fisher, E.C., Herries, A.I.R.,
556 Brown, K., Williams, H.M., Bernatchez, J., Ayalon, A., Nilssen, P.J., 2010. A high
557 resolution and continuous isotopic speleothem record of paleoclimate and
558 paleoenvironment from 90 to 53 ka from Pinnacle Point on the south coast of South
559 Africa. Quaternary Science Reviews 29, 2131-2145.
560 Birks, H.J.B., 1995. Quantitative palaeoenvironmental reconstructions, In: Maddy, D.,
561 Brew, J.S. (Eds.), Statistical Modelling of Quaternary Science Data. Quaternary
562 Research Association, Technical Guide 5, Cambridge, pp. 161-254.
563 Bronk Ramsey, C., 2013. OxCal 4.2 http://c14.arch.ox.ac.uk/.
564 Campbell, T.L., Lewis, P.J., Thies, M.L., Williams, J.K., 2012. A Geographic Information
565 Systems (GIS)-based analysis of modern South African rodent distributions, habitat
566 use, and environmental tolerances. Ecology and Evolution 2, 2881-2894.
567 Campbell, T.L., Lewis, P.J., Williams, J.K., 2011. Analysis of the modern distribution of
568 South African *Gerbilliscus* (Rodentia: Gerbillinae) with implications for Plio-
569 Pleistocene palaeoenvironmental reconstruction. South African Journal of Science
570 107, Article #497, 498 pages.
571 Chase, B.M., 2010. South African palaeoenvironments during marine oxygen isotope
572 stage 4: a context for the Howiesons Poort and Still Bay industries. Journal of
573 Archaeological Science 37, 1359-1366.
574 Chase, B.M., Boom, A., Carr, A.S., Carré, M., Chevalier, M., Meadows, M.E., Pedro,
575 J.B., Stager, J.C., Reimer, P.J., 2015a. Evolving southwest African response to

576 abrupt deglacial North Atlantic climate change events. Quaternary Science Reviews
577 121, 132-136.
578 Chase, B.M., Boom, A., Carr, A.S., Meadows, M.E., Reimer, P.J., 2013. Holocene
579 climate change in southernmost South Africa: rock hyrax middens record shifts in
580 the southern westerlies. Quaternary Science Reviews 82, 199-205.
581 Chase, B.M., Chevalier, M., Boom, A., Carr, A.S., 2017. The dynamic relationship
582 between temperate and tropical circulation systems across South Africa since the
583 last glacial maximum. Quaternary Science Reviews 174, 54-62.
584 Chase, B.M., Faith, J.T., Mackay, A., Chevalier, M., Carr, A.S., Boom, A., Lim, S.,
585 Reimer, P.J., 2018. Climatic controls on Later Stone Age human adaptation in
586 Africa's southern Cape. Journal of Human Evolution 114, 35-44.
587 Chase, B.M., Lim, S., Chevalier, M., Boom, A., Carr, A.S., Meadows, M.E., Reimer,
588 P.J., 2015b. Influence of tropical easterlies in southern Africa's winter rainfall zone
589 during the Holocene. Quaternary Science Reviews 107, 138-148.
590 Chase, B.M., Meadows, M.E., 2007. Late Quaternary dynamics of southern Africa's
591 winter rainfall zone. Earth-Science Reviews 84, 103-138.
592 Chase, B.M., Quick, L.J. 2018. Influence of Agulhas forcing of climate change in South
593 Africa’s southern Cape. Quaternary Research.
594 Chase, B.M., Thomas, D.S.G., 2007. Multiphase late Quaternary aeolian sediment
595 accumulation in western South Africa: timing and relationship to palaeoclimatic
596 changes inferred from the marine record. Quaternary International 166, 29-41.

Chevalier, M., Chase, B.M., 2015. Southeast African records reveal a coherent shift from high- to low-latitude forcing mechanisms along the east African margin across last glacial–interglacial transition. Quaternary Science Reviews 125, 117-130.

Chevalier, M., Chase, B.M., 2016. Determining the drivers of long-term aridity variability: a southern African case study. Journal of Quaternary Science 31, 143-151.

Clark, P.U., Dyke, A.S., Shakun, J.D., Carlson, A.E., Clark, J., Wohlfarth, B., Mitrovica, J.X., Hostetler, S.W., McCabe, A.M., 2009. The Last Glacial Maximum. Science, 710-714.

Cockcroft, M.J., Wilkinson, M.J., Tyson, P.D., 1987. The application of a present-day climate model to the Late Quaternary in southern Africa. Climatic Change 10, 161-181.

Copeland, S.R., Cawthra, H.C., Fisher, E.C., Lee-Thorp, J.A., Cowling, R.M., le Roux, P.J., Hodgkins, J., Marean, C.W., 2016. Strontium isotope investigation of ungulate movement patterns on the Pleistocene Paleo-Agulhas Plain of the Greater Cape Floristic Region, South Africa. Quaternary Science Reviews 141, 65-84.

Cowling, R.M., 1983. Phytochorology and vegetation history in the south-eastern Cape, South Africa. Journal of Biogeography 10, 393-419.

Deacon, H.J., 1979. Excavations at Boomplaas cave - a sequence through the Upper Pleistocene and Holocene in South Africa. World Archaeology 10, 241-257.

Deacon, H.J., Deacon, J., Scholtz, A., Thackeray, J.F., Brink, J.S., 1984. Correlation of palaeoenvironmental data from the Late Pleistocene and Holocene deposits at Boomplaas Cave, southern Cape, In: Vogel, J.C. (Ed.), Late Cainozoic Palaeoclimates of the Southern Hemisphere. Balkema, Rotterdam, pp. 339-351.

620 Deacon, J., 1984. The Later Stone Age of southernmost Africa. British Archaeological
621 Reports, International Series 213, Oxford.
622 Deacon, J., Lancaster, N., 1988. Late Quaternary Palaeoenvironments of Southern
623 Africa. Oxford University Press, New York.
624 Faith, J.T., 2013a. Taphonomic and paleoecological change in the large mammal
625 sequence from Boomplaas Cave, Western Cape, South Africa. Journal of Human
626 Evolution 65, 715-730.
627 Faith, J.T., 2013b. Ungulate diversity and precipitation history since the Last Glacial
628 Maximum in the Western Cape, South Africa. Quaternary Science Reviews 68, 191-
629 199.
630 Faith, J.T., Thompson, J.C., 2013. Fossil evidence for seasonal calving and migration of
631 extinct blue antelope (*Hippotragus leucophaeus*) in southern Africa. Journal of
632 Biogeography 40, 2108-2118.
633 Fernández-Jalvo, Y., Andrews, P., Denys, C., Sesé, C., Stoetzel, E., Marin-Monfort, E.,
634 Pesquero, D., 2016. Taphonomy for taxonomists: Implications of predation in small
635 mammal studies. Quaternary Science Reviews 139, 138-157.
636 Fick, S.E., Hijmans, R.J., 2017. WorldClim 2: new 1-km spatial resolution climate
637 surfaces for global land areas. International Journal of Climatology.
638 Fischer, H., Fundel, F., Ruth, U., Twarloh, B., Wegner, A., Udisti, R., Becagli, S.,
639 Castellano, E., Morganti, A., Severi, M., Wolff, E.W., Littot, G.C., Röthlisberger, R.,
640 Mulvaney, R., Hutterli, M.A., Kaufmann, P.R., Federer, U., Lambert, F., Bigler, M.,
641 Hansson, M.E., Jonsell, U., de Angelis, M., Boutron, C.F., Siggaard-Andersen, M.-L.,
642 Steffensen, J.P., Barbante, C., Gaspari, V., Gabrielli, P., Wagenbach, D., 2007.

643 Reconstruction of millennial changes in dust emission, transport and regional sea ice
644 coverage using the deep EPICA ice cores from the Atlantic and Indian Ocean sector
645 of Antarctica. Earth and Planetary Science Letters 260, 340-354.
646 Fisher, E.C., Bar-Matthews, M., Jerardino, A., Marean, C.W., 2010. Middle and Late
647 Pleistocene paleoscape modeling along the southern coast of South Africa.
648 Quaternary Science Reviews 29, 1382-1398.
649 Grayson, D.K., 1984. Quantitative Zooarchaeology. Academic Press, Orlando, Florida.
650 Happold, D., 2013. Mammals of Africa. Volume III: Rodents, Hares and Rabbits.
651 Bloomsbury Publishing, London.
652 Happold, M., Happold, D., 2013. Mammals of Africa. Volume IV: Hedgehogs, Shrews
653 and Bats. Bloomsbury Publishing, London.
654 Heine, K., 1982. The main stages of the late Quaternary evolution of the Kalahari
655 region, southern Africa. Palaeoecology of Africa 15, 53-76.
656 Hijmans, R.J., Cameron, S.E., Parra, J.L., Jones, P.G., Jarvis, A., 2005. Very high
657 resolution interpolated climate surfaces for global land areas. International Journal of
658 Climatology 25, 1965-1978.
659 Hogg, A.G., Hua, Q., Blackwell, P.G., Niu, M., Buck, C.E., Guilderson, T.P., Heaton,
660 T.J., Palmer, J.G., Reimer, P.J., Reimer, R.W., Turney, C.S.M., Zimmerman, S.R.H.,
661 2013. SHCal13 Southern Hemisphere Calibration, 0–50,000 Years cal BP.
662 Radiocarbon 55, 1889-1903.
663 Inskeep, R.R., 1987. Nelson Bay Cave, Cape Province, South Africa: the Holocene
664 levels. BAR International Series 357, Oxford.

665 Klein, R.G., 1972. Preliminary report on the July through September 1970 excavations
666 at Nelson Bay Cave, Plettenberg Bay (Cape Province, South Africa). Palaeoecology
667 of Africa 6, 177-208.
668 Klein, R.G., 1983. Palaeoenvironmental implications of Quaternary large mammals in
669 the fynbos region, In: Deacon, H.J., Hendey, Q.B., Lambrechts, J.J.N. (Eds.),
670 Fynbos Palaeoecology: A Preliminary Synthesis, South African National Scientific
671 Programmes Report No 75. Mills Litho, Cape Town, pp. 116-138.
672 Klein, R.G., 1991. Size variation in Cape dune molerat (*Bathyergus suillus*) and late
673 Quaternary climatic change in the southwestern Cape Province, South Africa.
674 Quaternary Research 36, 243-256.
675 Klein, R.G., Cruz-Uribe, K., 2016. Large mammal and tortoise bones from Elands bay
676 Cave (South Africa): implications for Later Stone Age environment and ecology.
677 South African Humanities 29, 259-282.
678 Le, J., Shackleton, N.J., 1994. Reconstruction paleoenvironment by transfer function:
679 model evaluation with simulated data. Marine Micropaleontology 24, 187-199.
680 Legendre, P., Legendre, L., 2012. Numerical Ecology. Elsevier, New York.
681 Loftus, E., Sealy, J., Lee-Thorp, J., 2016. New radiocarbon dates and Bayesian models
682 for Nelson Bay Cave and Byneskranskop 1: implications for the South African Later
683 Stone Age sequence. Radiocarbon 58, 365-381.
684 Lyman, R.L., 2008. Quantitative Paleozoology. Cambridge University Press,
685 Cambridge.
686 Lyman, R.L., 2012. The influence of screen mesh size, and size and shape of rodent
687 teeth on recovery. Journal of Archaeological Science 39, 1854-1861.

688 Lyman, R.L., 2017. Paleoenvironmental reconstruction from faunal remains: ecological
689 basics and analytical assumptions. Journal of Archaeological Research 25, 315-371.
690 Marean, C.W., 2010. Pinnacle Point Cave 13B (Western Cape Province, South Africa)
691 in context: The Capr Floral kingdom, shellfish, and modern human origins. Journal of
692 Human Evolution 59, 425-443.
693 Marean, C.W., Cawthra, H.C., Cowling, R.M., Esler, K.J., Fisher, E., Milewski, A., Potts,
694 A.J., Singels, E., De Vynck, J., 2014. Stone Age people in a changing South African
695 Greater Cape Floristic Region, In: Allsopp, N., Colville, J.F., Verboom, G.A. (Eds.),
696 Fynbos: Ecology, Evolution, and Conservation of a Megadiverse Region. Oxford
697 University Press, Oxford, pp. 164-199.
698 Matthews, T., Rector, A.L., Jacobs, Z., Herries, A.I.R., Marean, C.W., 2011.
699 Environmental implications of micromammals accumulated close to the MIS 6 to MIS
700 5 transition at Pinnacle Point Cave 9 (Mossel Bay, Western Cape Province, South
701 Africa). Paleogeography, Paleoclimatology, Paleoecology 302, 213-229.
702 Meadows, M.E., Baxter, A.J., 2001. Holocene vegetation history and
703 palaeoenvironments at Klaarfontein Springs, Western Cape, South Africa. The
704 Holocene 11, 699-706.
705 Meadows, M.E., Baxter, A.J., Parkington, J., 1996. Late Holocene environments at
706 Verlorenvlei, Western Cape Province, South Africa. Quaternary International 33, 81-
707 95.
708 Nel, T.H., Henshilwood, C.S., 2016. The small mammal sequence from the c. 76 – 72
709 ka Still Bay levels at Blombos Cave, South Africa – Taphonomic and
710 palaeoecological implications for human behaviour. PLoS ONE 11, e0159817.

711 Nel, T.H., Wurz, S., Henshilwood, C.S., 2018. Small mammals from Marine Isotope
712 Stage 5 at Klasies River, South Africa—Reconstructing the local palaeoenvironment.
713 Quaternary International 471, 6-20.
714 Pargeter, J., Loftus, E., Mackay, A., Mitchell, P.J., Stewart, B.A., In Press. New ages
715 from Boomplaas Cave, South Africa, provide increased resolution on late/terminal
716 Pleistocene human behavioural variability. Azania: Archaeological Research in
717 Africa.
718 Parkington, J.E., Cartwright, C., Cowling, R.M., Baxter, A., Meadows, M., 2000.
719 Palaeovegetation at the last glacial maximum in the western Cape, South Africa:
720 wood charcoal and pollen evidence from Elands Bay Cave. South African Journal of
721 Science 96, 543-546.
722 Partridge, T.C., Avery, D.M., Botha, G.A., Brink, J.S., Deacon, J., Herbert, R.S., Maud,
723 R.R., Scholtz, A., Scott, L., Talma, A.S., Vogel, J.C., 1990. Late Pleistocene and
724 Holocene climatic change in southern Africa. South African Journal of Science 86,
725 302-306.
726 Quick, L.J., Carr, A.S., Meadows, M.E., Boom, A., Bateman, M.D., Roberts, D.L.,
727 Reimer, P.J., Chase, B.M., 2015. A late Pleistocene-Holocene multi-proxy record of
728 palaeoenvironmental change from Still Bay, southern Cape Coast, South Africa.
729 Journal of Quaternary Science 30, 870-885.
730 Quick, L.J., Meadows, M.E., Bateman, M.D., Kirsten, K.L., Mäusbacher, R., Haberzettle,
731 T., Chase, B.M., 2016. Vegetation and climate dynamics during the last glacial
732 period in the fynbos-afrotemperate forest ecotone, southern Cape, South Africa.
733 Quaternary International 404B, 136-149.

734 Reed, D.N., 2005. Taphonomic implications of roosting behavior and trophic habits in
735 two species of African owl. Journal of Archaeological Science 32, 1669-1676.
736 Scholtz, A., 1986. Palynological and Palaeobotanical Studies in the Southern Cape, MA
737 Thesis, University of Stellenbosch, South Africa.
738 Schweitzer, F.R., Wilson, M.L., 1982. Byneskranskop 1, a late Quaternary living site in
739 the southern Cape Province, South Africa. Annals of the South African Museum 88,
740 1-203.
741 Scott, L., Woodborne, S., 2007a. Pollen analysis and dating of late Quaternary faecal
742 deposits (hyraceum) in the Cederberg, Western Cape, South Africa. Review of
743 Paleobotany and Palynology 144, 123-134.
744 Scott, L., Woodborne, S., 2007b. Vegetation history inferred from pollen in Late
745 Quaternary faecal deposits (hyraceum) in the Cape winter-rain region and its
746 bearing on past climates in South Africa. Quaternary Science Reviews 26, 941-953.
747 Sealy, J., Lee-Thorp, J., Loftus, E., Faith, J.T., Marean, C.W., 2016. Late Quaternary
748 environmental change in the Southern Cape, South Africa, from stable carbon and
749 oxygen isotopes in faunal tooth enamel from Boomplaas Cave. Journal of
750 Quaternary Science 31, 919-927.
751 Sealy, J.C., 1996. Seasonality of rainfall around the last glacial maximum as
752 reconstructed from carbon isotope analyses of animal bones from Nelson Bay Cave.
753 South African Journal of Science 92, 441-444.
754 Stuut, J.-B.W., Crosta, X., van der Borg, K., Schneider, R.R., 2004. On the relationship
755 between Antactic sea ice and southwestern African climate during the late
756 Quaternary. Geology 32, 909-912.

757 Talma, A.S., Vogel, J.C., 1992. Late Quaternary palaeotemperatures derived from a
758 speleothem from Cango Caves, Cape Province, South Africa. Quaternary Research
759 37, 203-213.
760 Taylor, I. (1994). Barn Owls. Cambridge University Press, Cambridge.
761 Thackeray, J.F., 1987. Late Quaternary environmental changes inferred from small
762 mammalian fauna, southern Africa. Climatic Change 10, 285-305.
763 Thackeray, J.F., 1990. Temperature indices from late Quaternary sequences in South
764 Africa: comparisons with the Vostok core. South African Geographic Journal 72, 47-
765 49.
766 Thackeray, J.F., Fitchett, J.M., 2016. Rainfall seasonality captured in micromammalian
767 fauna in Late Quaternary contexts, South Africa. Palaeontologia Africana 51, 1-9.
768 Trabucco, A., Zomer, R.J., 2009. Global Aridity Index (Global-Aridity) and Global
769 Potential Evapo-Transpiration (Global-PET) Geospatial Database. CGIAR
770 Consortium for Spatial Information, http://www.cgiar-csi.org/.
771 Tyson, P.D., 1986. Climatic change and variability in southern Africa. Oxford University
772 Press, Cape Town.
773 UNEP, 1997. World Atlas of Desertification. UNEP, London.
774 Van Andel, T.H., 1989. Late Pleistocene sea levels and the human exploitation of the
775 shore and shelf of southern South Africa. Journal of Field Archaeology 16, 133-155.
776 van Zinderen Bakker, E.M., 1967. Upper Pleistocene stratigraphy and Holocene
777 ecology on the basis of vegetation changes in Sub-Saharan Africa, In: Bishop,
778 W.W., Clark, J.D. (Eds.), Background to Evolution in Africa. University of Chicago
779 Press, Chicago, pp. 125-157.

van Zinderen Bakker, E.M., 1976. The evolution of late Quaternary paleoclimates of southern Africa. Palaeoecology of Africa 9, 160-202.

Vogel, J.C., Fuls, A., Ellis, R.P., 1978. The geographical distribution of Kranz grasses in South Africa. South African Journal of Science 74, 209-215.

Wilson, D.E., Reeder, D.M., 2005. Mammal Species of the World, 3rd Edition. Johns Hopkins University Press.

Zomer, R.J., Bossio, D.A., Trabucco, A., Yuanjie, L., Gupta, D.C., Singh, V.P., 2007. Trees and Water: Smallholder Agroforestry on Irrigated Lands in Northern India. International Water Management Institute, Columbo, Sri Lanka.

Zomer, R.J., Trabucco, A., Bossio, D.A., van Straaten, O., Verchot, L.V., 2008. Climate change mitigation: a spatial analysis of global land suitability for clean develoment mechanism afforestation and reforestation. Agriculture, Ecosystems and Environments 126, 67-80.

794 **FIGURE CAPTIONS**
795

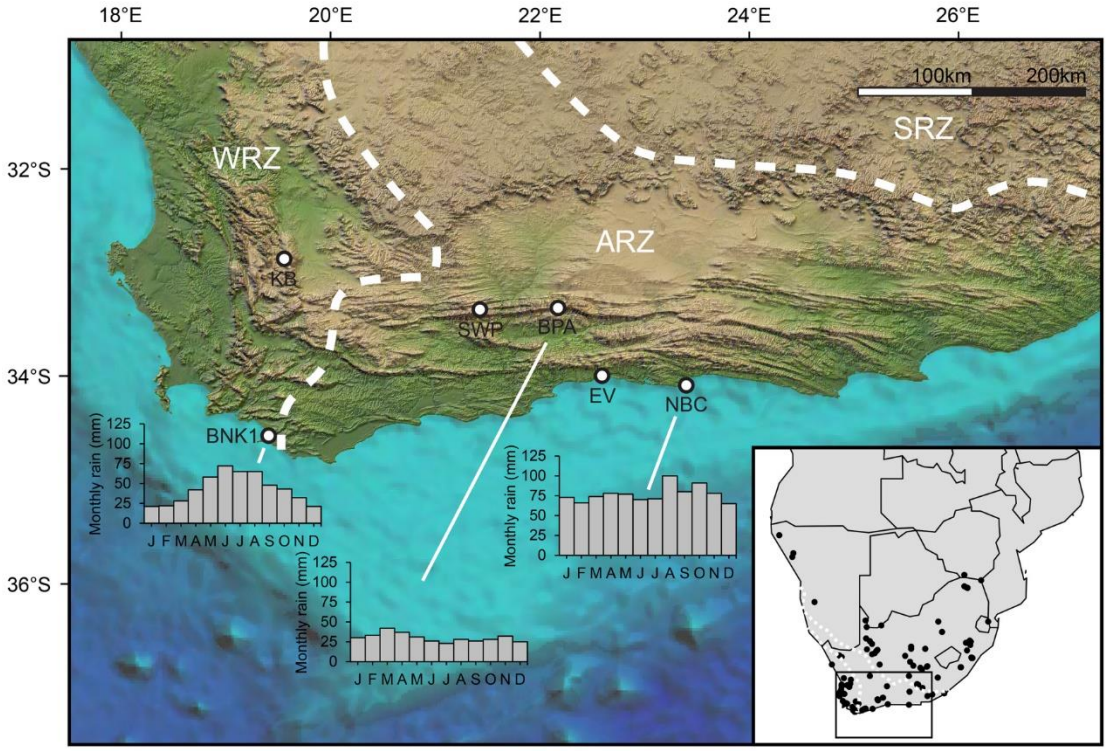

796
797

798 **Figure 1.** The location of the three fossil sites examined here, with monthly rainfall
799 totals (data from Hijmans et al. 2005), and other sites discussed in the text. BNK1 =
800 Byneskranskop 1; BPA = Boomplaas Cave; KB = Katbakkies Pass; NBC = Nelson Bay
801 Cave; SWP = Seweweekspoort. Inset: The location of 123 modern microfaunal samples
802 across southern Africa. Dashed white lines denote boundaries of winter rainfall zone
803 (WRZ), aseasonal rainfall zone (ARZ), and summer rainfall zone (SRZ).
804

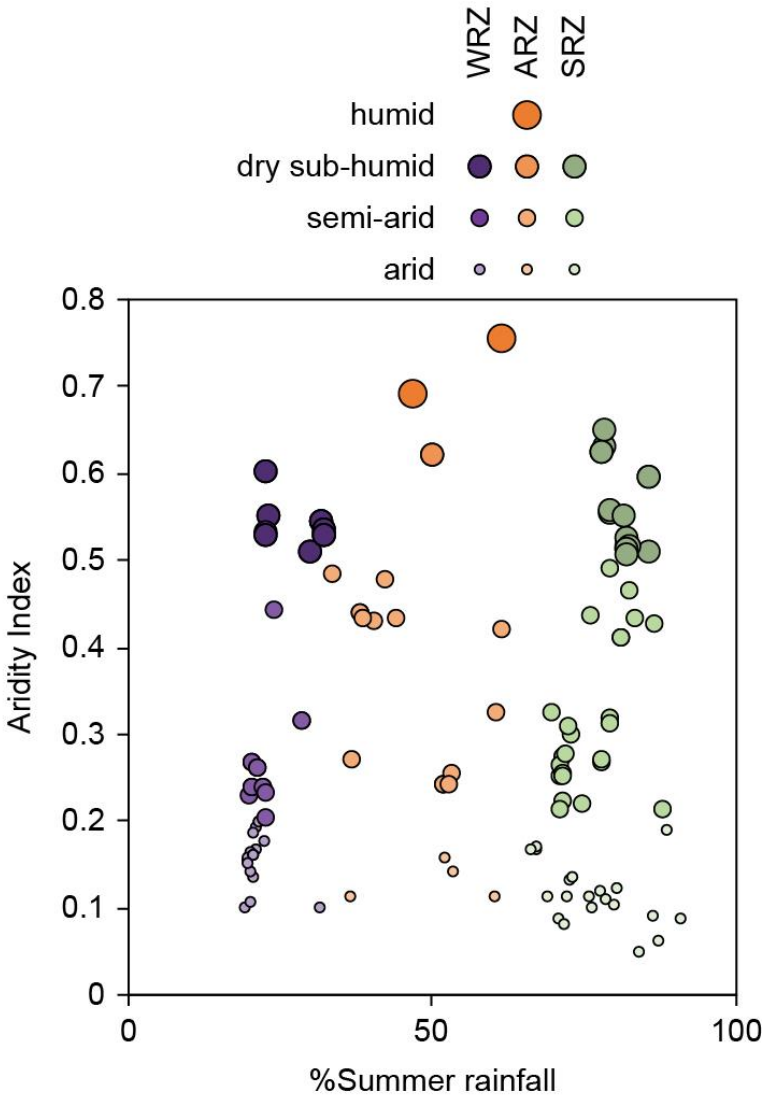

Figure 2. The percentage of summer rainfall (% of rainfall from October to March) and aridity index (AI) values (= MAP / MAE; from Zomer et al., 2007; Zomer et al., 2008; Trabucco and Zomer, 2009) of the 123 modern microfauna samples. Higher AI values indicate more humid conditions. Humid = AI > 0.65; Dry sub-humid = 0.5 < AI < 0.65; Semi-arid = 0.2 < AI < 0.5; Arid = 0.05 < AI < 0.2. WRZ = winter rainfall zone; ARZ = aseasonal rainfall zone; SRZ = summer rainfall zone.

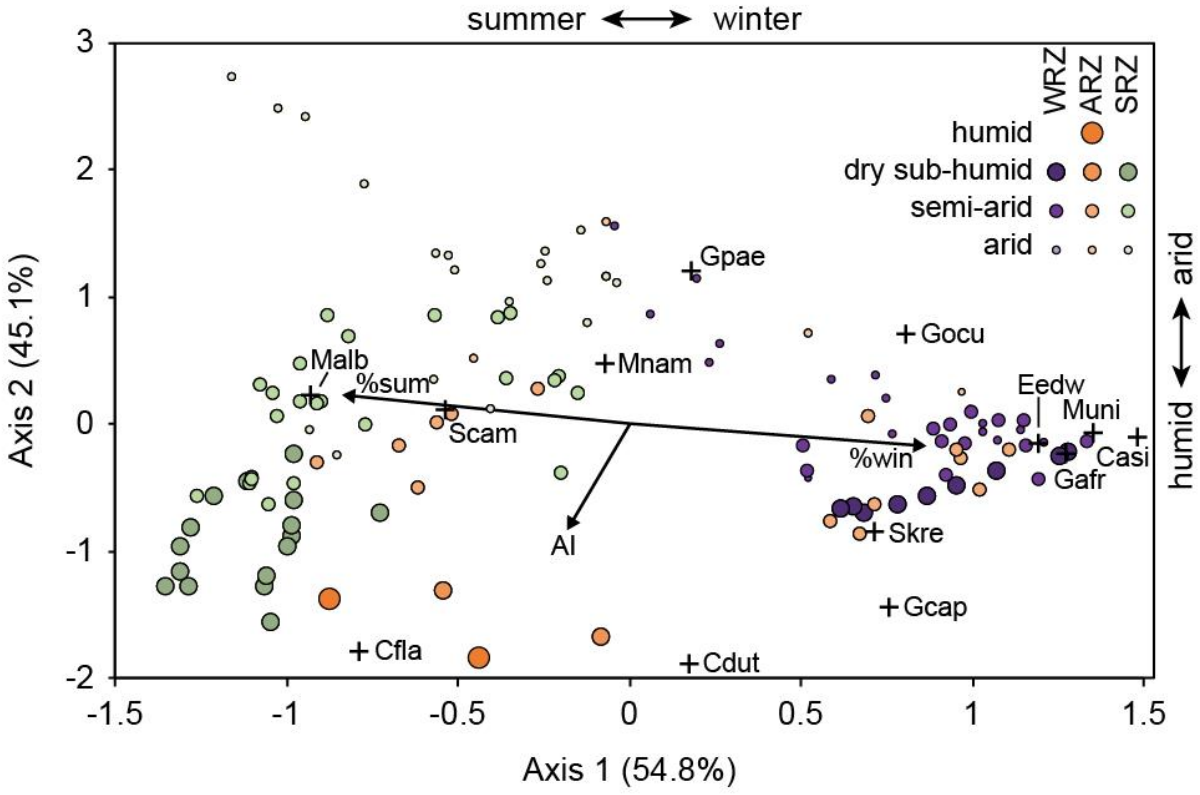

814

815

816 **Figure 3.** Ordination of modern assemblages (circles) and taxa (+) along the first two
817 axes of the CCA. Arrows indicate vectors for the aridity index (AI), %warm-quarter
818 rainfall (%sum), and %cold-quarter rainfall (%win). For the sake of clarity, only those
819 taxa occurring in the late Quaternary fossil samples are illustrated here (see
820 Supplementary Table 4 for all taxa). Species abbreviations are as follows: Cdut =
821 *Chlorotalpa duthiae*; Casi = *Chrysochloris asiatica*; Cfla = *Crocidura flavescens*; Eedw =
822 *Elephantulus edwardii*; Gcap = *Georychus capensis*; Gafr = *Gerbilliscus afra*; Gpae =
823 *Gerbillurus paeba*; Gocu = *Graphiurus ocularis*; Malb = *Mystromys albicaudatus*; Mnam
824 = *Micaleamys namaquensis*; Muni = *Myotomys unisulcatus*; Scam = *Saccostomus*
825 *campestris*; Skre = *Steatomys krebsii*

826

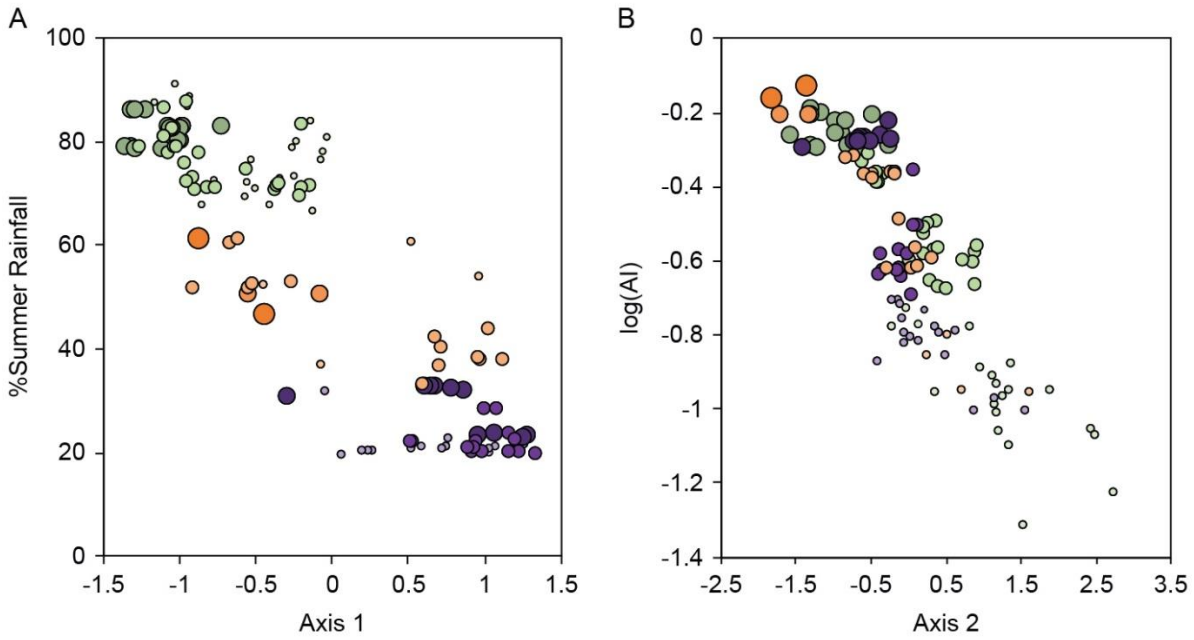

827

828 **Figure 4.** (A) The relationship between Axis 1 and the %summer rainfall, and (B) the
829 relationship between Axis 2 and the logarithm of the aridity index (AI) across the 123
830 modern microfaunal assemblages. Symbol legend for modern assemblages follows
831 Figure 2 (green = SRZ; orange = ARZ; purple = WRZ; larger symbols = more humid;
832 smaller symbols = more arid).

833

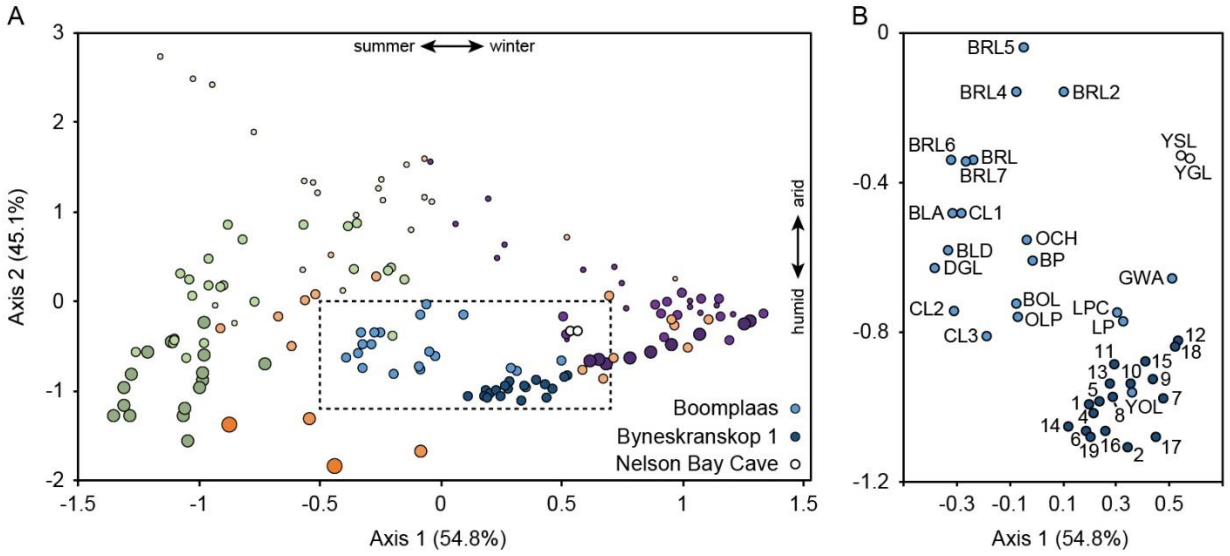

834

835 **Figure 5.** (A) Ordination of fossil assemblages relative to the modern assemblages.

836 Symbol for modern assemblages follows Figure 2 (green = SRZ; orange = ARZ; purple

837 = WRZ; larger symbols = more humid; smaller symbols = more arid). Box

838 encompassing fossil assemblages shown in B, with modern assemblages removed for

839 clarity.

840

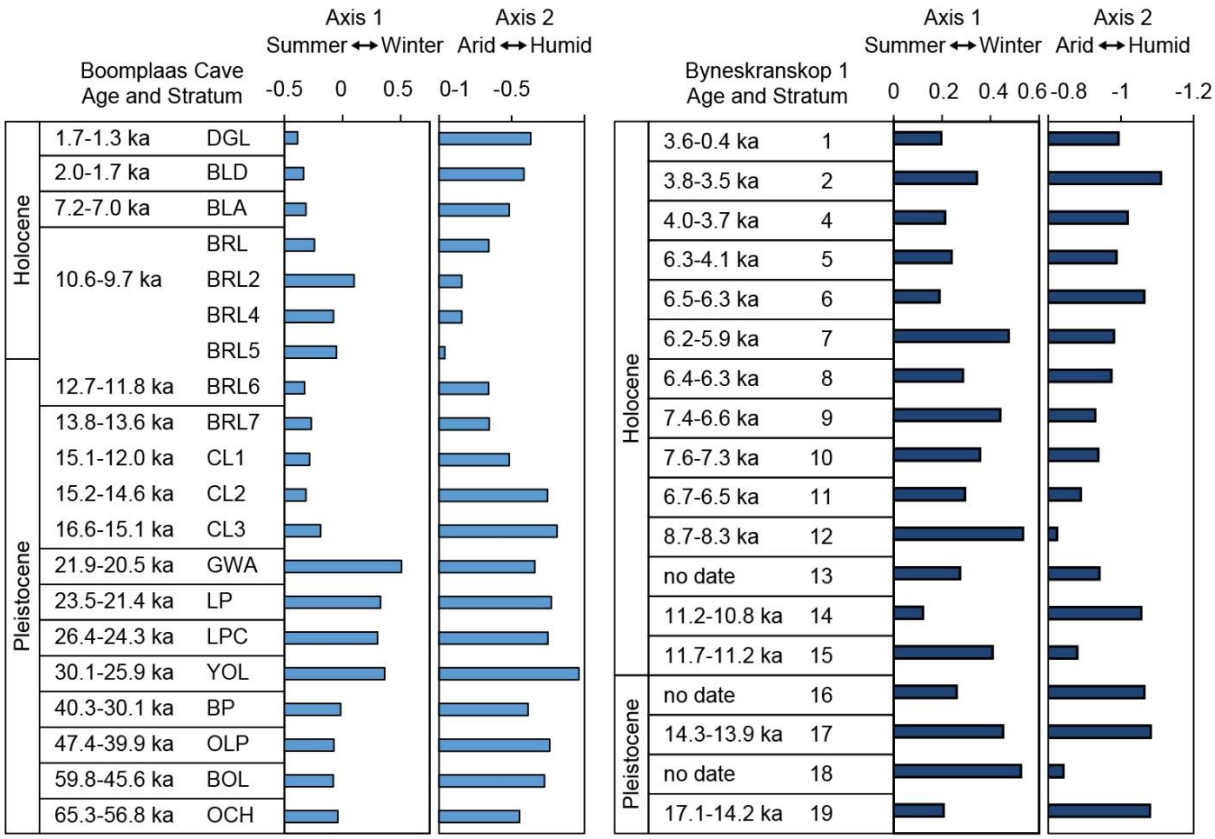

Figure 6. Axis 1 (rainfall seasonality) and axis 2 (aridity) scores through the Boomplaas Cave and Byneskranskop 1 sequences.. Ages for CL3 and up represent calibrated 2σ ranges of all ^{14}C ages in a given stratum, using SHCal13 (Hogg et al., 2013) calibration data and OxCal 4.3 (Bronk Ramsey, 2009). Ages for GWA and below are modelled age estimates from Pargeter et al. (2018).

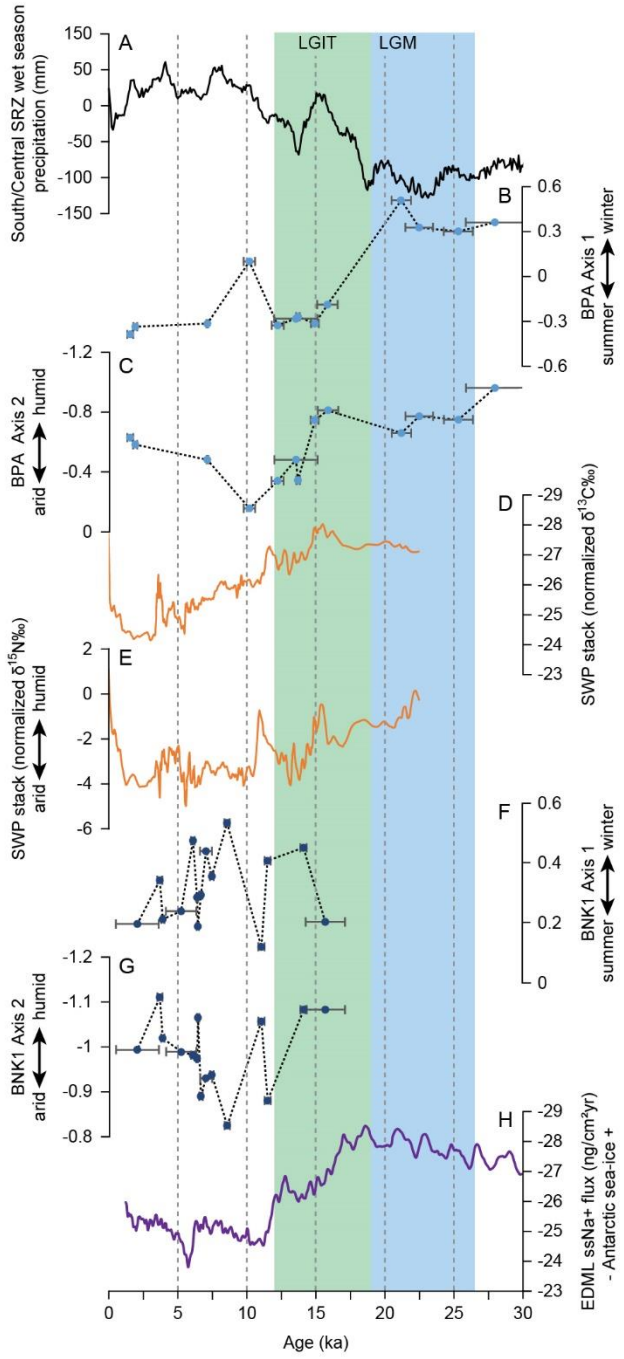

848

849 **Figure 7.** Comparison of precipitation seasonality (axis 1) and aridity (axis 2)

850 reconstructions from Boomplaas Cave (BPA: B, C) and Byneskranskop 1 (BNK1: F, G)

851 to local and regional proxy records, including (A) southern-central summer rainfall zone

852 (SRZ) wet season precipitation (Chevalier and Chase, 2015), (D) $\delta^{13}C$ and (E) $\delta^{15}N$

853 stacks from the Seweweekspoort hyrax middens (Chase et al. 2017, 2018), and (H)
854 sea-salt sodium flux from the EDML ice core indicating Antarctic sea-ice extent (Fischer
855 et al. 2007). Undated fossil assemblages are not plotted here. Error bars for microfauna
856 assemblages correspond to age ranges reported in Figure 6.
857